chemistry proceedings

MDPI

Proceedings

Synthesis of Myrtenal through Allylic Oxidation of α-Pinene over a Pd/SeO_2/SiO_2 Catalyst †

Florencia Antonella Musso [1], Victoria Soledad Gutierrez [2], María Alicia Volpe [2] and María Belén Faraoni [1,*]

[1] Instituto de Química del Sur (INQUISUR), Universidad Nacional del Sur—CONICET, Bahía Blanca, Argentina
[2] Planta Piloto de Ingeniería Química (PLAPIQUI), Universidad Nacional del Sur—CONICET, Bahía Blanca, Argentina
* Correspondence:Correspondence: bfaraoni@criba.edu.ar

Received: date; Accepted: date; Published: date

Abstract: SeO_2 based samples are tested for the oxidation of α-pinene, in liquid phase employing ethanol as the solvent. Commercial SeO_2 was tested both, under reflux and under 6 atm O_2 pressure. At conversion levels of approximately 40%, the yield to myrtenal was much higher in the latter (34.4%) than in the former case (18.0%) due to the high oxidant species availability. Besides the high yield is attained at relatively short reaction time. A palladium promoted selenium dioxide supported catalyst (Pd/SeO_2/SiO_2) was prepared, characterized and submitted to the catalytic test. Selenium dioxide (14.4%) was strongly fixed to the silica support. Upon the palladium introduction (0.98%) the reducibility of SeO_2 is modified, which originates a selenium species activation towards the allylic oxidation. A 12% conversion level is attained over Pd/SeO_2/SiO_2 following 8 h of reaction time, employing ethanol as the solvent at 134 °C. The main product is myrtenal, obtained with a selectivity of 62%. Over oxidation products are not detected. The palladium/selenium dioxide sample is easy to handle with and its recuperation following the reaction in liquid phase is possible.

Keywords: myrtenal; myrtenol; allylic oxidation; selenium dioxide; palladium

1. Introduction

Natural products oxidation plays an important role in the synthesis of new compounds, giving rise to new functional groups. In the case of allylic oxidations, the positions adjacent to double or triple bonds, lead to the corresponding α,β-unsaturated carbonyl compounds. There are several reports on allylic oxidations methodologies, being the most know the one employing selenium dioxide (SeO_2), mainly due to its relatively high regio- and chemoselectivity, leading mainly to the corresponding allylic alcohols or α,β-unsaturated carbonyl compounds [1–3].

In spite of SeO_2 is quite simple material to handle with, it presents some disadvantages: (i) stoichiometric relations or even high SeO_2/substrate ratios are employed for carry out the oxidations [4], (ii) long reaction times are required [5], (iii) moderate yields are obtained [5] and (iv) colloidal selenium species are formed during the reaction, which are difficult to separate from the reactive mixture [3–5].

Considering the above-mentioned drawbacks, and in the context of Green Chemistry Principles which promote the employment of heterogeneous catalysis for replacing stoichiometric process [6], it is interesting to study catalytic allylic oxidation reactions.

In the present work, the allylic oxidation of α-pinene is studied, since this monoterpene is one of the most abundant in natural sources and it is easily obtained from the essential oils of coniferous trees (pines), rosemary, lavender, and turpentine [7,8].

A wide variety of heterogeneous catalysts have been employed for carrying out the allylic oxidation of α-pinene, employing molecular oxygen. Rauchdi et al. have studied stabilized Ru nanoparticles suspensions, with water as the solvent and in tert-butyl hydroperoxide (TBHP) presence [9]. The authors have reported a relatively high yield to verbenone (39%). Platinum, palladium, ruthenium, rhodium and iridium metal catalysts supported on activated carbon have also been studied for the oxidation of α-pinene, but the introduction of nitrogenated admixtures was employed for increasing the yields to verbenone and verbenol [10]. Kholdeeva et al. have studied α-pinene oxidation over Cr- and Fe-MOF, employing TBHP. The authors reported conversion not higher than 22% at long reaction times (16 h), obtaining a mixture of several oxidation products [11]. The present work deals with the preparation and characterization of a Pd/SeO_2 supported catalyst, and its evaluation in the oxidation of α-pinene. The catalytic test is carried out in batch conditions, with O_2 as the oxidant and without employing initiators neither admixtures. The activity and the selectivity to the different products are measured and the reuse of the catalyst is analysed. The characterization is carried out by Transmission Electronic Spectroscopy (TEM), Fourier Transform Infrared Spectroscopy (FTIR), X-Ray Diffraction (XRD) and Temperature-programmed Reduction (TPR).

2. Experimental

2.1. Catalyst Synthesis and Characterization

A commercial sample of selenium dioxide (Merck, 98.0%) was employed for carrying out the reaction. This sample is named as SeO_2.

A silica supported selenium dioxide catalyst (SeO_2/SiO_2) was prepared from the wet impregnation method [12]. Approximately 0.3 g of SeO_2 were dissolved in absolute ethanol (99.5%, Cicarelli), at 40 °C under magnetic stirring for 24 h. The support was silica (SiO_2) from Davison, with a specific surface area of 210 m^2/g, was added to the selenium solution. Following the evaporation of ethanol, the sample was calcined at 400 °C during 60 min. The SeO_2/SiO_2 sample contains a nominal loading of 15 wt% of SeO_2.

A silica supported binary palladium/selenium dioxide catalyst was also prepared. A toluene solution of $Pd(AcAc)_2$ (Aldrich, 99.9%) was added to the SeO_2/SiO_2 catalyst. Following 24 h, the solid was filtered and the sample was calcined at 400 °C during 60 min. This catalyst is named as $Pd/SeO_2/SiO_2$ and contains a nominal Pd concentration of 1 wt%. Pd loading is determined by Atomic Absorption Spectroscopy in an A-Analyst Perkin Elmer equipment.

The samples were analyzed by X-ray diffraction (XRD) with a Panalytical Empyrean 3 diffractometer using Ni-filtered CuKα radiation and a PIXcel^{3D} detector, operated at a voltage of 45 kV and a current of 40 mA, in the 2θ range from 10° to 80°, using a continuous scan mode with a scan angular speed of 0.02° min^{-1}.

The samples were characterized by Fourier Transform Infrared Spectroscopy (FTIR) in a Nicolet Nexus apparatus. The spectra were obtained with a resolution of 2 cm^{-1} using 50 scans.

The palladium particle sizes were determined with Transmission Electronic Microscope (TEM), TEM JEOL 100 CX, at 100 kV. The Digital Micrograph software was employed for measuring crystal sizes.

2.2. Liquid Phase Oxidation of α-Pinene

Two different methodologies were followed for carrying out the oxidation of α-pinene (Riedel de Haden, 97%): (**i**) a methodology usually employed in Organic Synthesis. 1 eq of α-pinene in absolute ethanol (35 mL) was put in contact with 2.5 eq of SeO_2. The reaction mixture was placed in a round-bottomed flask and was heated under reflux until the disappearance of the starting material. (**ii**) a methodology usually followed for testing heterogeneous catalysis. The allylic oxidation reaction was conducted in a 50 mL Parr Instrument, operated in batch mode, at 134 °C and the pressure was raised to 6 atmospheres of oxygen. The stirring was set in 620 rpm and the reaction was carried out over SeO_2. For this case, the reactive mixture was: 1 eq of α-pinene and 2.5 eq of SeO_2 in 35 mL of absolute ethanol (0.02 M). The stirrer was switched on and the reaction is considered to be started.

Besides, also following (ii), the allylic oxidation reaction was conducted over the SeO_2/SiO_2 (200 mg) and over the $Pd/SeO_2/SiO_2$ (400 mg) catalysts in an ethanolic solution of α-pinene, 35 mL, 0.1M.

3. Results and Discussion

3.1. Preparation and Characterization

The selenium dioxide loading for both the SeO_2/SiO_2 and the $Pd/SeO_2/SiO_2$ was 14.4 wt%, which is a value quite similar to the target selenium dioxide concentration. In addition, it is observed that the amount of selenium dioxide remains constant following catalytic test. This result indicates that a strong selenium dioxide/silica support interaction is developed.

The palladium loading in the $Pd/SeO_2/SiO_2$ sample (0.98 wt%) is also similar to the nominal concentration (1 wt%).

In Figure 1, the XRD pattern corresponding to commercial SeO_2 sample and to the SeO_2/SiO_2 catalyst respectively are shown. The commercial sample shows diffraction peak assigned to selenium dioxide and to selenious acid (JCPDS card Nº 00-041-0259 and JCPDS card Nº 00-022-1314 for H_2SeO_3 and SeO_2 respectively). Both species are generally found together since hydration of the oxide leads to the acid. For the supported catalysts, a wide peak, due to silica is observed [13]. No peak corresponding to selenium species was detected, probably due to the fact that such species are highly dispersed on silica, and the corresponding peaks appear in the same region as the ones due to the support.

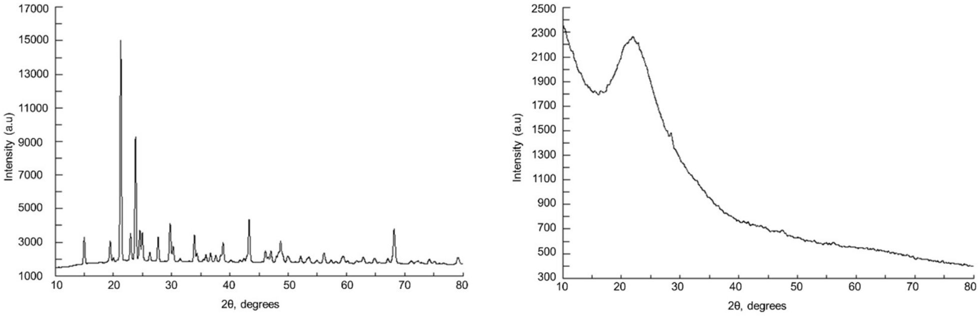

(**a**) (**b**)

Figure 1. XRD patterns of: (**a**) SeO_2; (**b**) SeO_2/SiO_2.

Both the fresh and the spent binary catalysts ($Pd/SeO_2/SiO_2$) were also studied by XRD. The corresponding patterns are shown in Figure 2. For the fresh sample, a similar spectrum as in the case of SeO_2/SiO_2 was obtained and the signals due to palladium or palladium oxide are not detected. The noble metal peaks are not observed probably due to the high dispersion of palladium crystals developed in this sample. On the other hand, it is interesting to note that the XRD results corresponding to the used catalyst, following the catalytic test, indicate the presence of signals due to metallic palladium at 39.5 and 47.3 degrees of $2\theta°$ and to palladium oxide (28.6 degrees of $2\theta°$). It is likely that palladium species are highly dispersed in the fresh catalyst and that following the liquid phase oxidation, a sintering of the noble metal crystals occurs, giving rise to larger palladium particles responsible for XRD peaks.

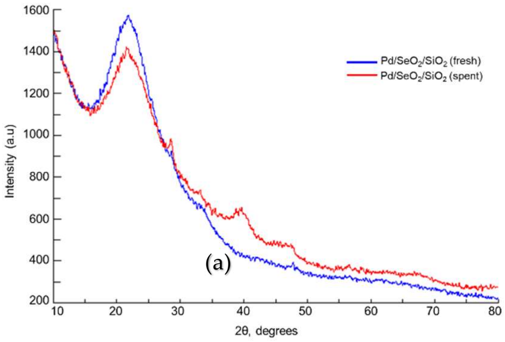

Figure 2. XRD pattern of: (**a**) fresh Pd/SeO_2/SiO_2 catalyst; (**b**) spent Pd/SeO_2/SiO_2 catalysts.

FTIR spectra corresponding to SeO_2, SiO_2 and SeO_2/SiO_2 are shown in Figure 3. For SeO_2 (Figure 3a), the bands at 871 and 668 cm^{-1} are due to Se-O stretching, while those at 1248 and 1150 cm^{-1} are due Se-OH [14].

FTIR spectrum corresponding to SiO_2 shows several bands (Figure 3b). Bands at 1190 and 1095 cm^{-1} are due to Si-O stretching [13]. Both of these bands are shifted and their relative intensity is modified in SeO_2/SiO_2. This modification would be due to the high interaction between both oxides. Besides, the band at 894 and 678 cm^{-1} due to selenium dioxide species are observed for the SeO_2/SiO_2 sample.

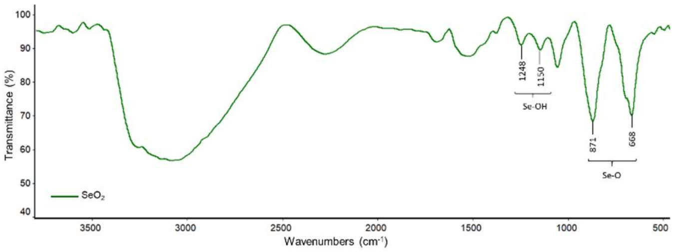

(**a**)

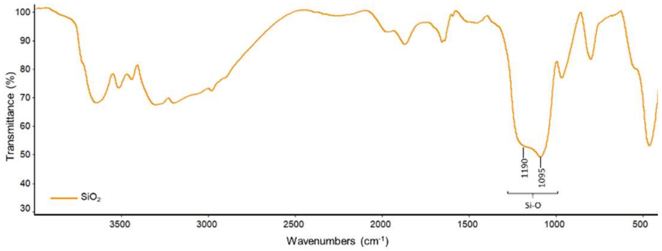

(**b**)

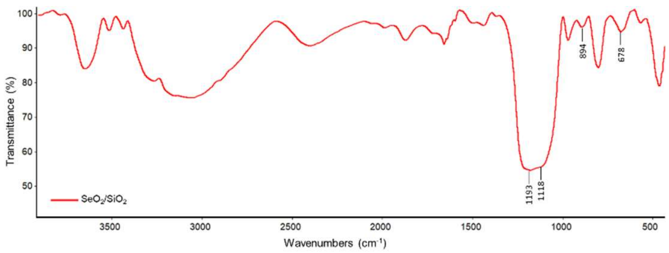

(**c**)

Figure 3. FTIR spectra of: (**a**) SeO_2; (**b**) SiO_2; (**c**) SeO_2/SiO_2.

The FTIR analysis of the $Pd/SeO_2/SiO_2$ catalyst showed similar result to the SeO_2/SiO_2 sample (Figure 4). The spent catalyst, following the catalytic test, was also studied by FTIR, and no differences with the fresh sample are detected. It is worth noting that bands due to C-H, C=O, or C-OH groups were not detected over the used sample, which would indicate that neither irreversible adsorption of reactants, intermediates nor products occurs during the reaction. Such adsorption was observed over used catalyst employed for liquid phase reactions involving aldehyde, alcohols, and acids over metal supported catalysts, and would be responsible for catalyst deactivation [15].

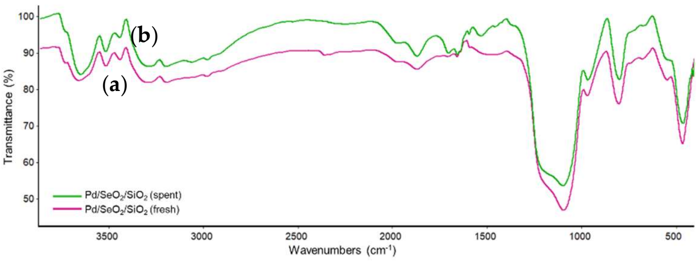

Figure 4. FTIR spectra of: (**a**) fresh $Pd/SeO_2/SiO_2$; (**b**) spent $Pd/SeO_2/SiO_2$.

Regarding TEM characterization was carried out over SeO_2/SiO_2 sample, but is not possible to observe any difference between the silica support and the selenium species. Similar electronic densities of the samples would be the responsible for the low contrast between silica and selenium species.

TEM analysis was also carried out for the $Pd/SeO_2/SiO_2$ catalyst, both for the as prepared sample and for the catalyst following the catalytic reaction. The results are shown in Figure 5. Palladium particles in the fresh sample present a particle size of 2.9 nm, while the ones corresponding to spent catalyst show crystals with a size of 3.5 nm. It is concluded that morphological modification takes place under reaction conditions, leading to an increase in palladium particle size. We will revert to this matter later.

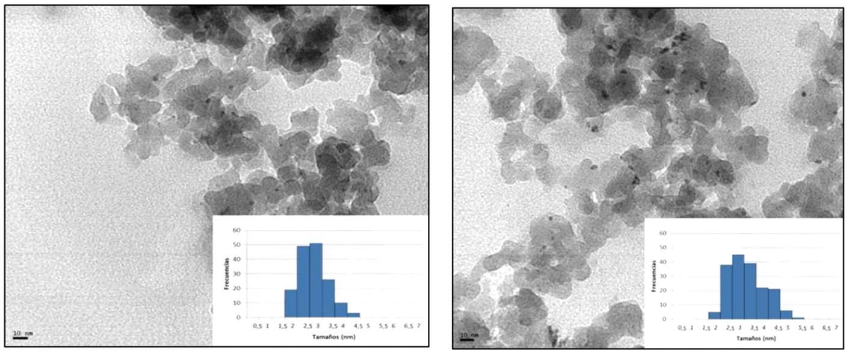

(**a**) (**b**)

Figure 5. TEM images of: (**a**) fresh Pd/SeO_2/SiO_2 catalysts; (**b**) spent Pd/SeO_2/SiO_2 catalysts.

3.2. Catalytic Test

In the scheme, shown in Figure 6 some of the possible products from the α-pinene allylic oxidation are shown.

Selenium dioxide mediates the allylic oxidation of alkenes with retention of the double bond position. When the double bond is inside a ring, oxidation occurs in the α-position to the more substituted carbon of the double bond with a reactivity order $CH_2 > CH_3 > CH$ [3]. Based on this, for α-pinene, myrtenal and myrtenol should be expected when employing SeO_2. Myrtenal is a component of essential oils found mainly in medicinal plants and has been reported to have pharmacological activities against many diseases such as diabetes, cancer, and malaria, among others [16–18]. On the other hand, antimicrobial and antifungal activities have been also documented [19]. Myrtenol, another monoterpene isolated from essential oils of some aromatic plants, although it is used for its flavouring properties, several studies have shown that it has anti-inflammatory and antinociceptive effects [20,21].

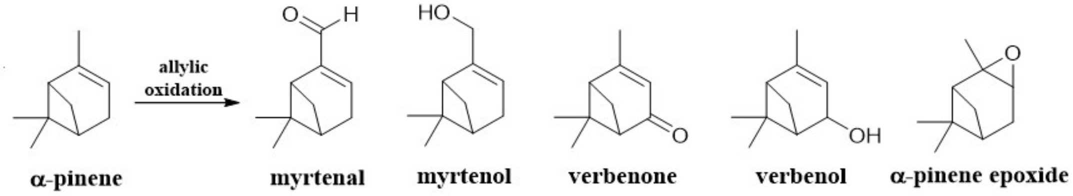

Figure 6. Some of the products from the allylic oxidation of α-pinene.

In the present work, the allylic oxidation of α-pinene over SeO_2 was carried out following two methodologies. Firstly (methdology i) the reaction was performed in liquid phase employing ethanol as the solvent, under reflux (78 °C), and conversion and selectivities were measured along with time. As could be expected myrtenol was the main product at early reaction times and low conversion values. Anyway, myrtenal was also produced (Table 1). Myrtenal yield increases along with time, while the one corresponding to myrtenol diminishes, showing that the aldehyde is being formed from the oxidation of the alcohol. At 13 h the selectivity to myrtenal does not surpass 56%, yielding 28%. This yield is lower than the one reported by Lin et al. [18], however it is important to note that these authors have carried out the reaction employing 1,4-dioxane, a solvent not friendly to the environment.

Table 1. Allylic oxidation of α-pinene over SeO_2 through conventional test (methodolgy (i), under reflux) [a].

Entry	Time (h)	X [b] (%)	S ol [c] (%)	S al [d] (%)
1	5	18	72	28
2	7	23	65	35
3	9	34	59	41
4	11	41	56	44
5	13	50	44	56

[a] Reaction conditions: 1 eq. of α-pinene, 2.5 eq. of SeO_2, in 35 mL of ethanol (0.02 M), 78 °C. [b] Conversion of α-pinene. [c] Selectivity to myrtenol. [d] Selectivity to myrtenal.

In addition, the oxidation of α-pinene was performed over SeO_2 following methodology (ii), in batch conditions, under oxygen pressure (6 atm) and at a higher temperature than in the previous case (134 °C against 78 °C). In this case, the 41% of conversion was attained at shorter times than for the reaction being carried out under reflux (5 h against 11 h). The only detected products were myrtenal and myrtenol, showing a notably high selectivity to the aldehyde (84%) (Table 2). Thus, the yield to myrtenal (34.4%) was higher when the reaction is carried out under oxygen pressure than under reflux (18%). The high yield to myrtenal reached in the former case would be due to both the higher reaction temperature and to the improved oxygen concentration in the liquid phase.

Table 2. Allylic oxidation of α-pinene over SeO_2 (methodolgy (ii), batch reactor under 6 atm O_2) [a].

Entry	Time (h)	X [b] (%)	S ol [c] (%)	S al [d] (%)
1	2	5	58	42
2	3.5	21	29	71
3	5	41	16	84

[a] Reaction conditions: 1 eq. of α-pinene, 2.5 eq. of SeO_2, in 35 mL of ethanol (0.02 M), 134 °C. [b] Conversion of α-pinene. [c] Selectivity to myrtenol. [d] Selectivity to myrtenal.

In the context of developing a supported heterogeneous catalyst, SeO_2 was fixed to SiO_2; thus the SeO_2/SiO_2 sample was obtained. This catalyst is practically inactive in the allylic oxidation of α-pinene, reaching a 3% conversion level following 18 h, at 134 °C under oxygen pressure (6 atm). It is likely that in the SeO_2/SiO_2 sample, the active species (selenium ones) are diluted in an inert support, resulting in an insufficient active phase amount. The introduction of Pd to the selenium dioxide/silica system was envisaged for increasing the activity of the SeO_2/SiO_2 catalyst. The promotion of the selenium dioxide/silica material with the noble metal was quite effective, since the $Pd/SeO_2/SiO_2$ catalyst is much more active than the palladium free sample, tested under the same experimental conditions. A 12% conversion was reached at 8 h, showing a relatively high selectivity to myrtenal (62%), being myrtenol the other product. It is important to note that no other co-product was detected.

The relatively high selectivity to myrtenal achieved over the $Pd/SeO_2/SiO_2$ catalyst is a quite interesting result, since previous reports, corresponding to Pd (or any other noble metal) based catalysts, indicated that the main products corresponding to α-pinene oxidations are verbenol and verbenone, and also that verbenoic acid is detected, originated in over oxidation of the aldehyde. It is likely that the oxidation over $Pd/SeO_2/SiO_2$ is governed by selenium species, leading to the allylic oxidation of the double bond in α position to the more substituted carbon of the double bond, and that palladium plays a promotional role on SeO_2.

In order to throw some light on the promotional effect of Pd on selenium dioxide, an analysis of the reducibility of the catalysts was carried out. TPR results (Figure 7) indicate that palladium strongly modifies the SeO_2 redox character. A change in the reduction pattern of supported selenium dioxide upon the noble metal introduction can be observed. In the profile corresponding to SeO_2/SiO_2 (Figure 7a) a consumption peak centred at 290 °C is detected, which would be due to the reduction of selenium dioxide. In the binary $Pd/SeO_2/SiO_2$ catalyst the reduction temperature is notably lower (Figure 7b), showing a reduction peak with a maximum at 270 °C. In this sense, it is proposed that the palladium promotional effect on selenium dioxide is originated by a high interaction which modifies the selenium dioxide reducibility. Taking in mind the catalytic results which indicate that the oxidation yields only myrtenal and myrtenol it is concluded that palladium just plays a promotional role, without a direct participation in the activation of α-pinene. On the other hand, if palladium would act as the active phase, verbenone and verbenol should be produced as usually observed over noble metal-based catalysts.

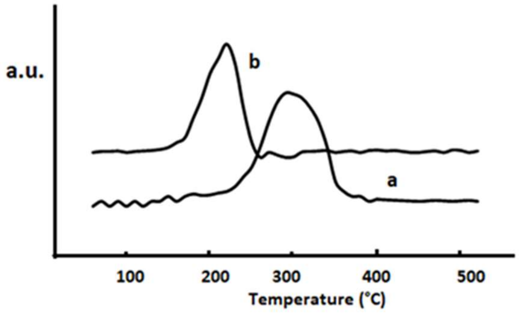

Figure 7. TPR profiles of: (**a**) SeO_2/SiO_2; (**b**) $Pd/SeO_2/SiO_2$.

It is concluded that $Pd/SeO_2/SiO_2$ is an active catalyst for carrying out the oxidation of α-pinene, which shows a relatively high selectivity towards myrtenal. In addition, a practical advantage arises due to the employment of a supported material, which is easy both to handle and to separate from the reactive mixture by comparison with the SeO_2 sample.

Finally, a comment on the reuse of the $Pd/SeO_2/SiO_2$ should be carried out. The spent catalyst, following the reaction, was withdrawn from the reactor, washed with fresh solvent a new catalytic test was performed. The activity of the catalyst was too low, showing that the reuse cannot be accomplished. Probably the deactivation phenomena over $Pd/SeO_2/SiO_2$ are related with the larger palladium particle size, as measured from TEM analysis. It could be speculated that larger Pd crystals have no the same promotional effect on SeO_2 due to a lower contact between palladium and selenium species. In on-going studies other catalysts, with different selenium dioxide and palladium loading are being prepared and tested for the interest reaction, trying to obtain a sample which can be reused.

4. Conclusions

The comparisons between two different methodologies for the oxidation of α-pinene, employing SeO_2, leads to different myrtenal yields. The reaction carried out under reflux, under traditional organic synthesis conditions, yields lower myrtenal than when the reaction is performed under 6 atm of O_2. At the same conversion level, the selectivity to myrtenal is higher under oxidant overpressure than under reflux.

An effective supported catalyst for the oxidation of α-pinene was studied. The binary Pd/SeO_2 catalyst supported on SiO_2 leads to the oxidation in the α position to the more substituted carbon of the double bond. The binary sample is more selective to myrtenal than unsupported selenium dioxide, showing no overoxidation products. The present results are promising regarding the substitution of the conventional oxidation methods for α-pinene by a catalytic transformation, in line with Green Chemistry Principles.

Acknowledgments: This work was supported by Consejo Nacional de Investigaciones Científicas y Técnicas (CONICET), grant number: PIP 11220150100107 to MAV; Universidad Nacional del Sur (UNS), grant number: PGI 24/Q105 and Agencia Nacional de Promoción Científica y Tecnológica (ANPCyT), grant number: PICT-2017-1443 to MBF. MAV and VSG are researcher members of CONICET. MBF is research member of CIC. FAM thanks the CONICET for a doctoral fellowship.

Conflicts of Interest: The authors declare no conflict of interest.

References

1. Nakamaura, A.; Nakada, M. Allylic oxidations in natural product synthesis. *Synthesis* **2013**, *45*, 1421–1451, doi:10.1055/s-0033-1338426.
2. Bulman, P.C.; McCarthy, T.J. Oxidation adjacent to C=C bonds. In *Comprehensive Organic Synthesis*, 1st ed.; Trost, B.M., Fleming, I., Eds.; Pergamon Press: Kidlington (Oxford), UK, 1991; Volume 7, pp. 83–117, doi:10.1016/B978-0-08-052349-1.00184-0.
3. Mlochowski, J.; Wójtowicz-Mlochowska, H. Developments in synthetic application of selenium (IV) oxide and organoselenium compounds as oxygen donors and oxygen-transfer agents. *Molecules* **2015**, *20*, 10205–10243, doi:10.3390/molecules200610205.
4. Lempers, H.E.B.; Sheldon, R.A. Allylic oxidation of olefins to the corresponding α,β-unsaturated ketones catalyzed by chromium aluminophosphate-5. *Appl. Catal. A* **1996**, *143*, 137–143, doi:10.1016/0926-860X(96)00076-2.
5. Tagawa, Y.; Yamashita, K.; Higuchi, Y.; Goto, Y. Improved oxidation of active methyl group of N-heteroaromatic compounds by selenium dioxide in the presence of tert-butyl hydroperoxide. *Heterocycles* **2003**, *60*, 953–957, doi:10.3987/COM-02-9702.
6. Sheldon, R.A.; Arends, I.; Hanefeld, U. *Green Chemistry and Catalysis*, 1st ed.; Wiley-VCH: Weinheim, Germany, 2007; pp. 1–43.
7. Noma, Y.; Asakawa, Y. Biotransformation of monoterpenoids by microorganisms, insects, and mammals. In *Handbook of Essential Oils: Science, Technology, and Applications*, 1st ed.; Can Baser, K.H., Buchbauer, G., Eds.; CCR Press: Boca Raton, FL, USA, 2010; Volume 1, pp. 585-736.
8. Noma, Y.; Asakawa, Y. Biotransformation of monoterpenoids. In *Comprehensive Natural Products II: Chemistry and Biology*, 1st ed.; Mander, L., Liu, H.W., Eds.; Elsevier: Kidlington (Oxford), UK, 2010; Volume 1, pp. 669-801, doi:10.1016/B978-008045382-8.00742-5.
9. Rauchdi, M.; Ali, M.A.; Roucoux, A.; Denicourt-Nowicki, A. Novel access to verbenone via ruthenium nanoparticles-catalyzed oxidation of α-pinene in neat water. *Appl. Catal. A* **2018**, *550*, 266–273, doi:10.1016/j.apcata.2017.11.016.
10. Kuznetsova, L.I.; Kuznetsova, N.I.; Lisitsyn, A.S.; Beck, I.E.; Likholobov, V.A.; Ancel, J.E. Liquid-phase oxidation of α-pinene with oxygen catalyzed by carbon-supported platinum metals. *Kinet. Catal* **2007**, *48*, 44–50, doi:10.1134/S0023158407010065.
11. Kholdeeva, O.A.; Skobelev, I.Y.; Ivanchikova, I.D.; Kovalenko, K.A.; Fedin, V.P.; Sorokin, A.B. Hydrocarbon oxidation over Fe- and Cr-containing metal-organicframeworks MIL-100 and MIL-101–a comparative study. *Catal. Today* **2014**, *238*, 54–61, doi:10.1016/j.cattod.2014.01.010.
12. Singh, J.; Sharma, M.; Kad, G.L.; Chhabra, B.R. Selective oxidation of allylic methyl groups over a solid support under microwave irradiation. *J. Chem. Res.* **1997**, *7*, 264–265, doi:10.1039/A700758B.
13. Khan, A.S.; Khalid, H.; Sarfraz, Z.; Khan, M.; Iqbal, J.; Muhammad, N.; Fareed, M.A.; ur Rehman, I. Vibrational spectroscopy of selective dental restorative materials. *Appl. Spectrosc. Rev.* **2016**, *52*, 507–540, doi:10.1080/05704928.2016.1244069.
14. Falk, M.; Giguére, P.A. Infrared spectra and structure of selenious acid. *Can. J. Chem* **1958**, *36*, 1680–1685, doi:10.1139/v58-244.
15. Piqueras, C.M.; Puccia, V.; Vega, D.A.; Volpe, M.A. Selective hydrogenation of cinnamaldehyde in supercritical CO_2 over Me–CeO_2 (Me = Cu, Pt, Au): Insight of the role of Me–Ce interaction. *Appl. Catal. B. Env* **2016**, *185*, 265–271, doi:10.1016/j.apcatb.2015.12.031.
16. Ayyasamy, R.; Leelavinothan, P. Myrtenal alleviates hyperglycaemia, hyperlipidaemia and improves pancreatic insulin level in STZ-induced diabetic rats. *Pharm. Biol.* **2016**, *54*, 2521–2527, doi:10.3109/13880209.2016.1168852.
17. Babu, L.H.; Perumal, S.; Balasubramanian, M.P. Myrtenal, a natural monoterpene, down-regulates TNF-α expression and suppresses carcinogen-induced hepatocellular carcinoma in rats. *Mol. Cell. Biochem* **2012**, *369*, 183–193, doi:10.1007/s11010-012-1381-0.
18. Lin, G.S.; Duan, W.G.; Yang, L.X.; Huang, M.; Lei, F.H. Synthesis and antifungal activity of novel myrtenal-based 4-methyl-1,2,4-triazole-thioethers. *Molecules* **2017**, *22*, 1–10, doi:10.3390/molecules22020193.
19. Burgueño-Tapia, E.; Zepeda, G.L.; Joseph-Nathan, P. Absolute configuration of (-)-myrtenal by vibrational circular dichroism. *Phytochemistry* **2010**, *71*, 1158–1161, doi:10.1016/j.phytochem.2010.04.005.

20. Gomes, B.S.; Neto, B.P.S.; Lopes, E.M.; Cunha, F.V.M.; Araújo, A.R.; Wanderley, C.W.S.; Wong, D.V.T.; Júnior, R.C.P.L.; Ribeiro, R.A.; Sousa, D.P.; et al. Anti-inflammatory effect of the monoterpene myrtenol is dependent on the direct modulation of neutrophil migration and oxidative stress. *Chem. Biol. Interact.* **2017**, *273*, 73–81, doi:10.1016/j.cbi.2017.05.019.
21. Silva, R.O.; Salvadori, M.S.; Sousa, F.B.M.; Santos, M.S.; Carvalho, N.S.; Sousa, D.P.; Gomes, B.S.; Oliveira, F.A.; Barbosa, A.L.R.; Freitas, R.M.; et al. Evaluation of the anti-inflammatory and antinociceptive effects of myrtenol, a plant derived monoterpene alcohol, in mice. *Flavour. Fragr. J.* **2014**, *29*, 184–192, doi:10.1002/ffj.3195.